Spectrochimica Acta Part B 65 (2010) 466–470

Contents lists available at ScienceDirect

Spectrochimica Acta Part B

journal homepage: www.elsevier.com/locate/sab

Study of copper surface oxidation by grazing angle X-ray excitation ☆

Héctor Jorge Sánchez [a,b,*], Carlos Alberto Pérez [c]

[a] Universidad Nacional de Córdoba — Córdoba CBA, Argentina
[b] CONICET, Argentina
[c] Laboratório Nacional de Luz Síncrotron — Campinas SP Brazil

ARTICLE INFO

Article history:
Received 14 October 2009
Accepted 23 February 2010
Available online 1 March 2010

Keywords:
TXRF
Depth profiling
Stratified media

ABSTRACT

This work reports measurements of copper surface oxidation by XRF analysis under grazing angle excitation. The mathematical model for analyzing data is based on the usual equation for XRF intensity, corrected by the stratified model for the layer excitation. The final expressions are fitted to the data by using the Simplex algorithm.

Three samples of silicon wafers with surface layers of copper were made by using the controlled-evaporation technique under vacuum. The final layer thicknesses were 190 Å, 400 Å, and 800 Å. For each sample, several measurements were carried out by performing an angular scan in the region of the critical angle for total reflection. Different measurements were taken immediately after evaporation, after 30 min, after 1 h, after 4 h, and after 30 min in oven at 65°.

The results show small variations among the different spectra measured for each sample. The most significant variations are observed for the first measurement (after evaporation) and the last one (after the heating in oven). The mathematical model works correctly for a two-layer scheme but shows inconsistencies for more complex schemes. This indicates that the stratified model is not appropriate for continuous media due to the nature of the theoretical assumptions in which the stratified model is based. Our results show also that the surface oxidation process takes place in the first moments of exposition to air and does not progress afterwards except if the sample is heated.

1. Introduction

The external total-reflection phenomenon in XRF analysis gave an important impulse to X-ray spectroscopy. It was first noted and used by Yoneda and Horiuchi [1] in 1971, giving place to a new experimental method in spectrochemical analysis, the so-called Total Reflection X-Ray Fluorescence technique (TXRF). Later, the technique was extended to the analysis of optically prepared surfaces and depth profiling by exciting the sample at grazing angles or detecting the fluorescent radiation emitted at grazing angles [2,3]. These techniques are known as Grazing Incidence X-Ray Fluorescence (GIXRF) and Grazing Emission X-Ray Fluorescence (GEXRF). The equivalence between GIXRF and GEXRF was demonstrated by using the Reciprocity Principle of Lorentz [4], showing that the algebraic equations and the fitting algorithms are essentially the same.

General depth profiling analysis involves all kinds of varying profiles, the most complex samples having a continuous variation of elemental composition or density with depth. For stratified media, the propagation of X-rays at grazing angles can be calculated by representing the sample as a stratified structure in order to obtain analytical solution of the problem [5,6]. The density of each layer is given by an average density of that layer, and many surface layers can be necessary for a correct representation of the sample. This involves a great number of mathematical operations and therefore an efficient calculation method of X-ray propagation at glancing angles is required. Several mathematical algorithms have been reported for the calculations of X-ray propagation at grazing angles in stratified media; some of them can be appreciated in Refs. [7–9].

Although the stratified model has been used to analyze continuum profiles, this model is not completely appropriate to this kind of medium. As it will be described in the next sections, some of the fundamental hypothesis of the theory of the propagation of electromagnetic waves in stratified media are not quite fulfilled. For continuous media the fundamental equations of XRF can be used including a new spatial variable (the depth). This variable appears in the parameter that takes into account the spatial (depth) profile. Perhaps, the most advanced and accurate method to deal with these equations was proposed by Smolders and Urbach in 2002 [10]. These authors made use of Laplace's transforms to solve the space-varying parameter. Nevertheless, this methodology is neither simple nor very precise; the main problem in the data treatment is the statistical noise of the experimental

☆ This paper was presented at the 13th Conference on Total Reflection X-Ray Fluorescence Analysis and Related Methods (TXRF 2009), held in Gothenborg, Sweden, 15–19 June 2009, and is published in the Special Issue of Spectrochimica Acta Part B, dedicated to that conference.

* Corresponding author. Universidad Nacional de Córdoba — Córdoba CBA, Argentina.
E-mail address: jsan@famaf.unc.edu.ar (H.J. Sánchez).

0584-8547/$ – see front matter © 2010 Elsevier B.V. All rights reserved.
doi:10.1016/j.sab.2010.02.018

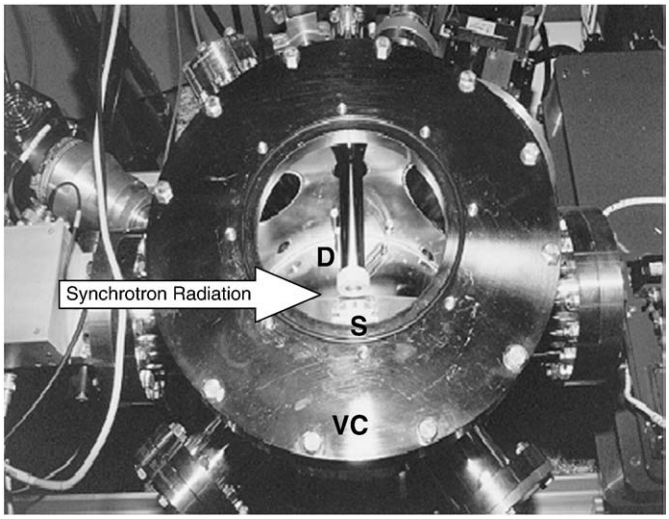

Fig. 1. Top view of the TXRF station of XRF beamline. The big arrow indicates the direction of the incident beam, *VC* denotes the chamber itself, *S* stands for the sample and sample holder, and *D* shows the head of the solid-state detector.

data and the small number of experimental points of a typical depth profiling experiment.

In this work, we present measurements of surface oxidation of cooper by Grazing Incidence XRF analysis. Some interesting results were obtained regarding the depth of the oxidation layer and the velocity of the oxidation. The experimental data were analyzed with a standard procedure for the analysis of stratified media and the results obtained showed a depth profile with very low spatial sensitivity. This fact is in agreement with failure of the hypothesis of the stratified model for continuous media.

2. Experimental

The sample preparations and measurements were carried out at the Laboratório Nacional de Luz Síncrotron, LNLS Campinas Brazil, in the Total-Reflection Station of the XRF beamline [11]. The electron energy inside the storage ring is 1.37 GeV with a dipole magnetic field of 1.65 T. This gives a critical photon energy of 2.08 keV. The natural emittance is 100 nm·rad and the revolution frequency is 3.2 MHz for this 93.2 m long machine.

The XRF beamline is equipped with a silicon (111) channel-cut monochromator. It consists of a monolithic crystal with a slot in order to expose two parallel surfaces. The white beam hits the first crystal face and reflects X-rays with wavelength λ, which satisfy the Bragg's condition. This monochromatized beam strikes the second crystal face, which reflects the beam along a parallel trajectory. Thus, as the crystal is rotated, the transmitted beam changes with a beam offset equal to $2/l\cos(\theta)$, being l the slot thickness and θ the Bragg angle. The crystal is located inside a high vacuum chamber, which is maintained below 10–6 mbar by using an ion pump. With this crystal, the energy can be tuned from 3 to 14 keV with a relative resolution of 3×10^{-4} between 7 and 10 keV. The photon flux was measured with a photodiode (IRD, Model AXUV-20HE1) with 100% efficiency between 100 eV and 12 keV and a whole active area of 20 mm^2. At 100 mA and 9 keV the measured photon flux was 3×10^{9} photons·s^{-1}.

The station consists of a vacuum chamber ($\sim5\times10^{-4}$ mbar working pressure) with a goniometer stage inside (Figs. 1 and 2). Fine rotation can be achieved by means of a high-resolution translation stage, coupled to a disc by a thin steel wire. The translation stage of 0.5 mm/step with a disc of 59 mm of radius produces a 10 mrad angular resolution. The positioning of the sample on the beam path can be done by using a UHV linear feedthrough, placed at the bottom of the chamber and coupled to the sample holder, and moving the whole experimental station on a slide. In both cases, the

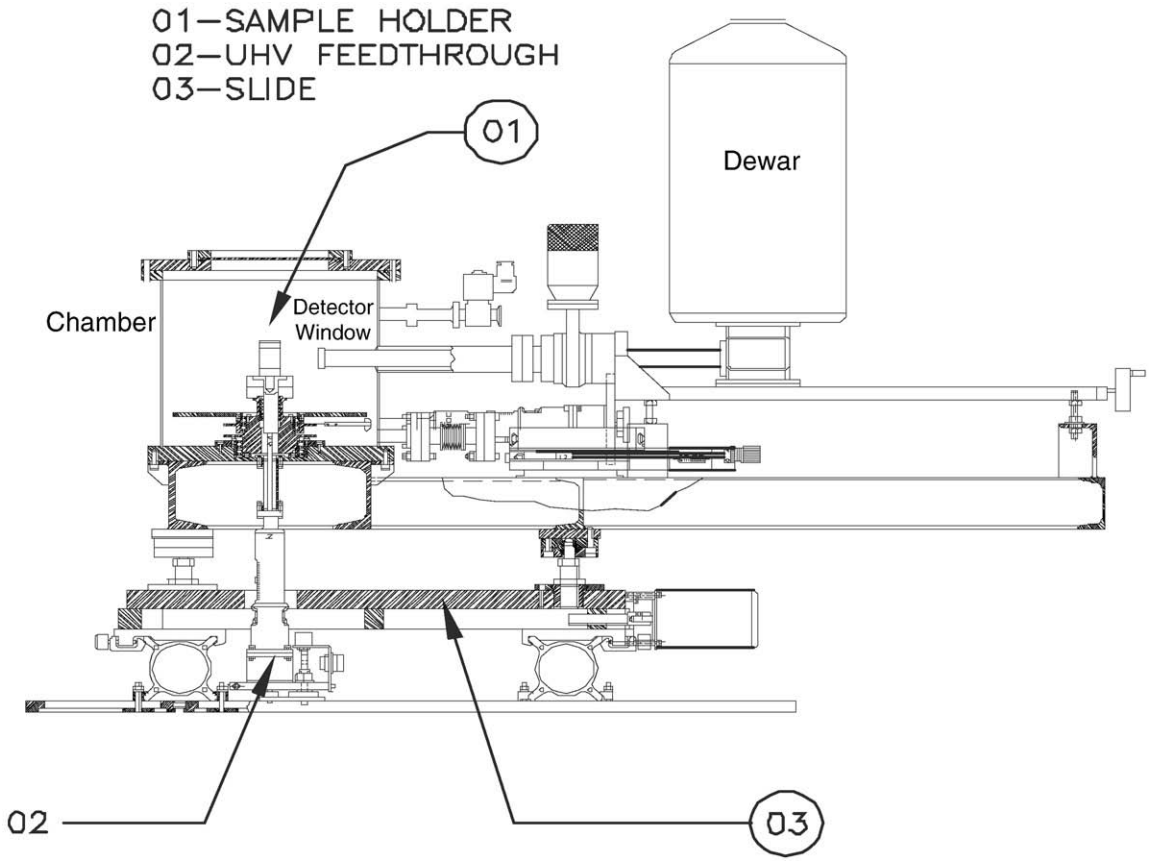

Fig. 2. Schematic of the TXRF station with the positioning stages.

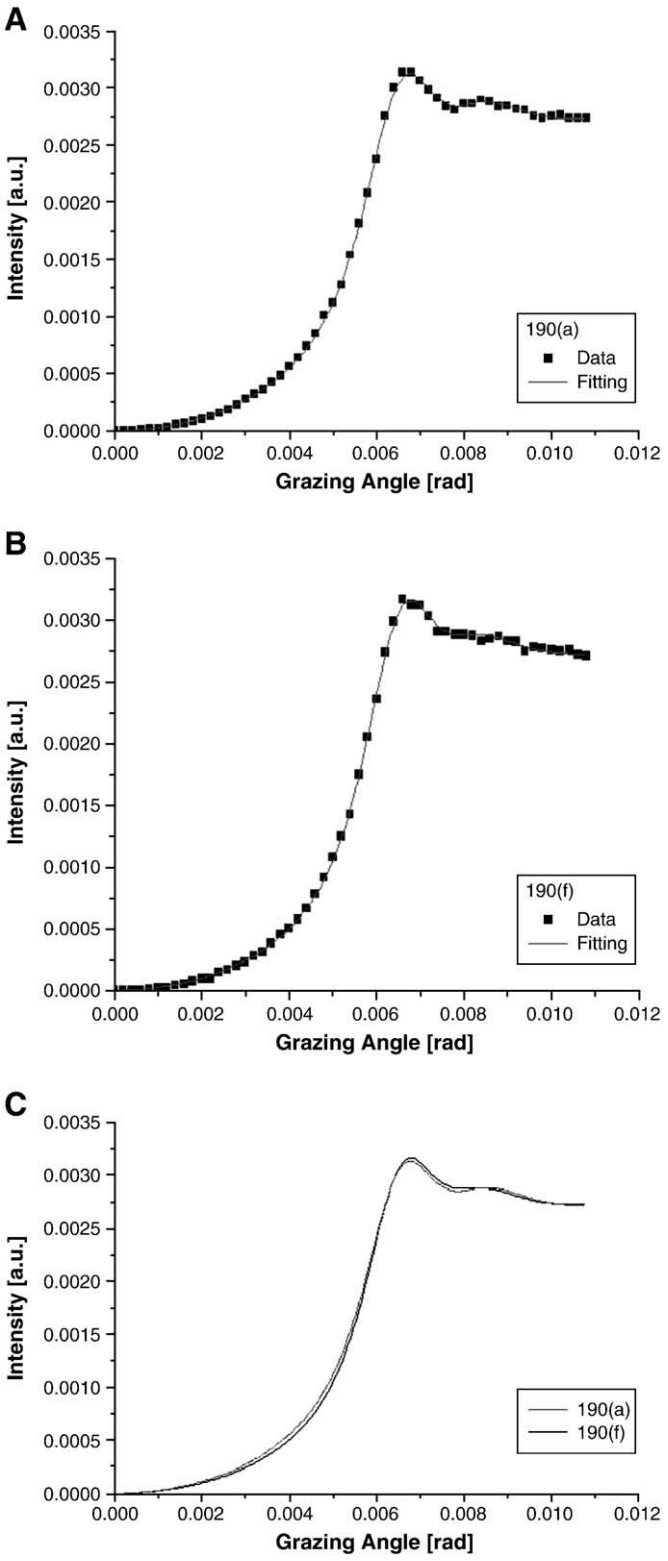

Fig. 3. (A) Experimental data of the sample with a surface layer of 190 Å, right after deposition. The solid line represents the fitting curve considering two layers. Layer 1: 5.9 g/cm³, 16 Å. Layer 2: 8.4 g/cm³, 180 Å. (B) Experimental data of the sample with a surface layer of 190 Å, after 30 min in oven at 65°. The solid line represents the fitting curve considering two layers. Layer 1: 6.3 g/cm³, 37 Å. Layer 2: 8.5 g/cm³, 168 Å. (C) A comparison of the fitted curves of (A) and (B).

precision on the movements is 2 μm. The total-reflection condition is achieved by means of remote-controlled translation and rotation stages. The detection system consisted of a Si(Li) solid-state detector with a Be window of 25 μm and a resolution of 148 eV at 5.9 keV located at 5 mm from the sample holder, the electronic chain consists of fast amplifier and a multichannel analyzer with a ADC of 25 μs of conversion time. In order to keep the detection limits under

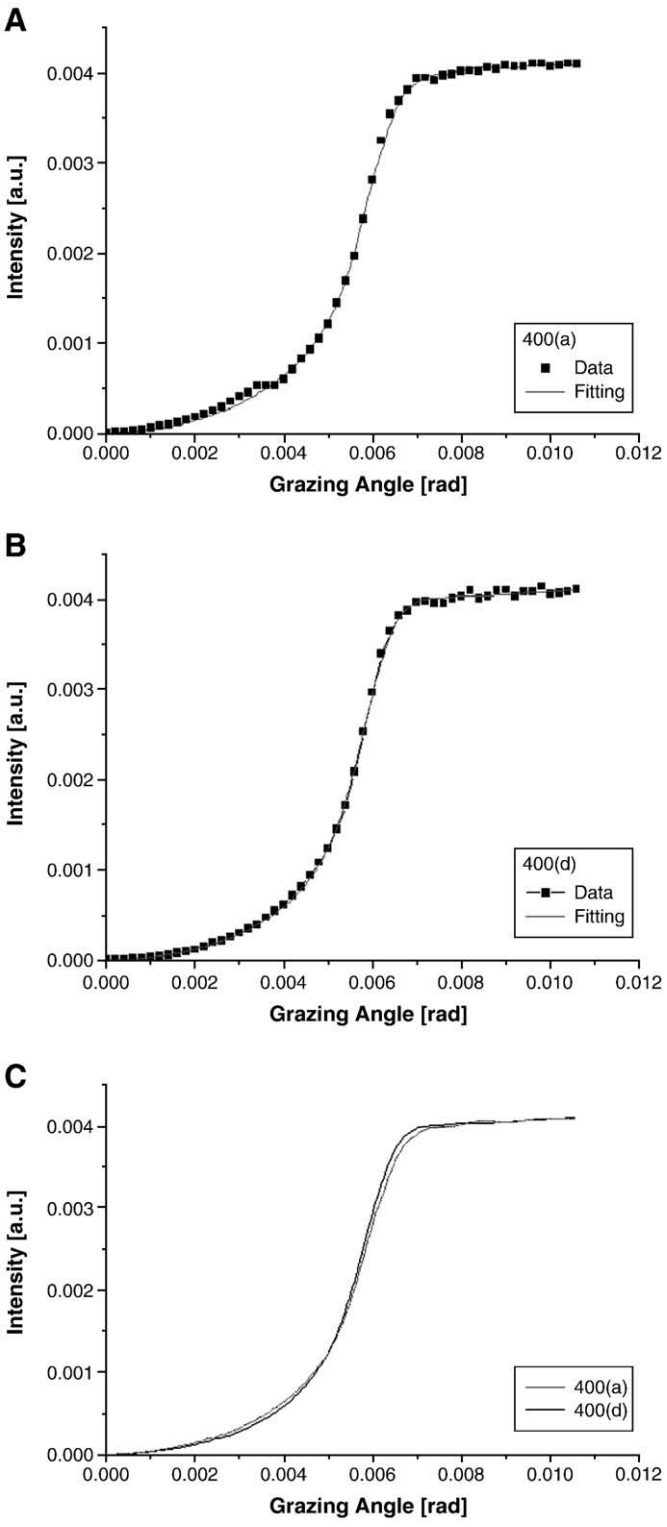

Fig. 4. (A) Experimental data of the sample with a surface layer of 400 Å, right after deposition. The solid line represents the fitting curve considering two layers. Layer 1: 4.6 g/cm³, 31 Å. Layer 2: 8.5 g/cm³, 378 Å. (B) Experimental data of the sample with a surface layer of 400 Å, after 30 min in oven at 65°. The solid line represents the fitting curve considering two layers. Layer 1: 4.9 g/cm³, 53 Å. Layer 2: 8.6 g/cm³, 356 Å. (C) A comparison of the fitted curves of (A) and (B).

reasonable values (less than 10%) a 1 mm collimator was located in front of the detector window.

Three samples of silicon wafers with surface layers of copper were made by using the controlled-evaporation technique under vacuum. According to the calibration of the evaporating system, the final thicknesses of the layers were 190 Å, 400 Å, and 800 Å. Samples were conserved in portable vacuum chambers until they were ready for measurements in order to prevent unwanted oxidation.

For each sample, several measurements were carried out by performing an angular scanning in the region of the critical angle for total reflection. An angular range between 0 and 12 mrad was covered with a measuring time of 10 s/point for approximately 60 points. Monochromatic photons of 9 keV were used to irradiate the sample in order to excite the copper K-edge. In this way, the Kα line of copper was measured and later analyzed to study its behavior near the critical angle of total reflection. Different measurements were taken immediately after evaporation, after 30 min, after 1 h, after 4 h, and after 30 min in oven at 65°.

3. Data analysis and results

The measurements show small variations among the different spectra measured for each sample. The most significant variations are observed for the first measurement (right after evaporation) and the last one (after the heating in oven at 65 °C). This indicates that a soft superficial oxidation is produced very fast, right after the first contact with air. Afterward, a more intense and deeper oxidation appears after heating. Figs. 3–5(A) show the experimental data obtained from the angular scannings around the critical angle of total reflection for the samples of 190 Å, 400 Å and 800 Å after evaporation. Figures in the center (B) show the experimental data for the same samples after heating.

These data were fitted using different models for the number of surface layers following the method of stratified media. Briefly, the measured fluorescent intensity is fitted to the theoretical expression [7,12]:

$$I_f = \int_0^{E_{max}} \int_0^{\infty} I_0(z,E) Q(z,E) M(z,E) \mathrm{d}z \mathrm{d}E$$

where $Q(z,E)$ is the emission factor, $M(z,E)$ takes into account the absorption effects, and $I_o(z,E)$ is the excitation intensity at depth z corrected by the stratification of the medium.

The key point in this treatment is to represent the factor $I_o(z,E)$. This factor takes into account the number of layers that the model uses to represent the depth profile of the surface. In this work we use the approach reported by Pérez et al. [13] that makes use of the properties of Hessenberg's matrices to transform a matricial system of equations into a scalar system of equations. In this way, the calculations are carried out very efficiently and with high precision.

Solid lines in Figs. 3–5(A and B) show the theoretical curves fitted to the experimental data. Figs. 3–5(C) show the fitted curves for these samples after evaporation and after heating. These analyses correspond to a two-layer model. Calculated values of density and depth are shown in the captions (for layer #1 and layer #2) and Table 1. As can be observed, the density of layer #1 corresponds approximately to copper oxide and the density of #2 corresponds approximately to pure copper.

Comparing the values before and after heating of the sample of 190 Å, the results are consistent as well as for the total amount of Cu on top of the Si substrate as for the sum of the thicknesses of the two layers. These two values almost don't change from one scan to another. The thickness of the oxide layer increases, the one of the second layer decreases indicating a further oxidation of Cu. This reflects the fact that copper is further oxidized by the heating treatment; the sum of the thickness of the two layers reproduces also quite well the nominal thickness of the evaporated Cu. The average densities are somewhat below the densities of Cu respectively oxidized Cu but this is usually the case for thin layers. In the case of

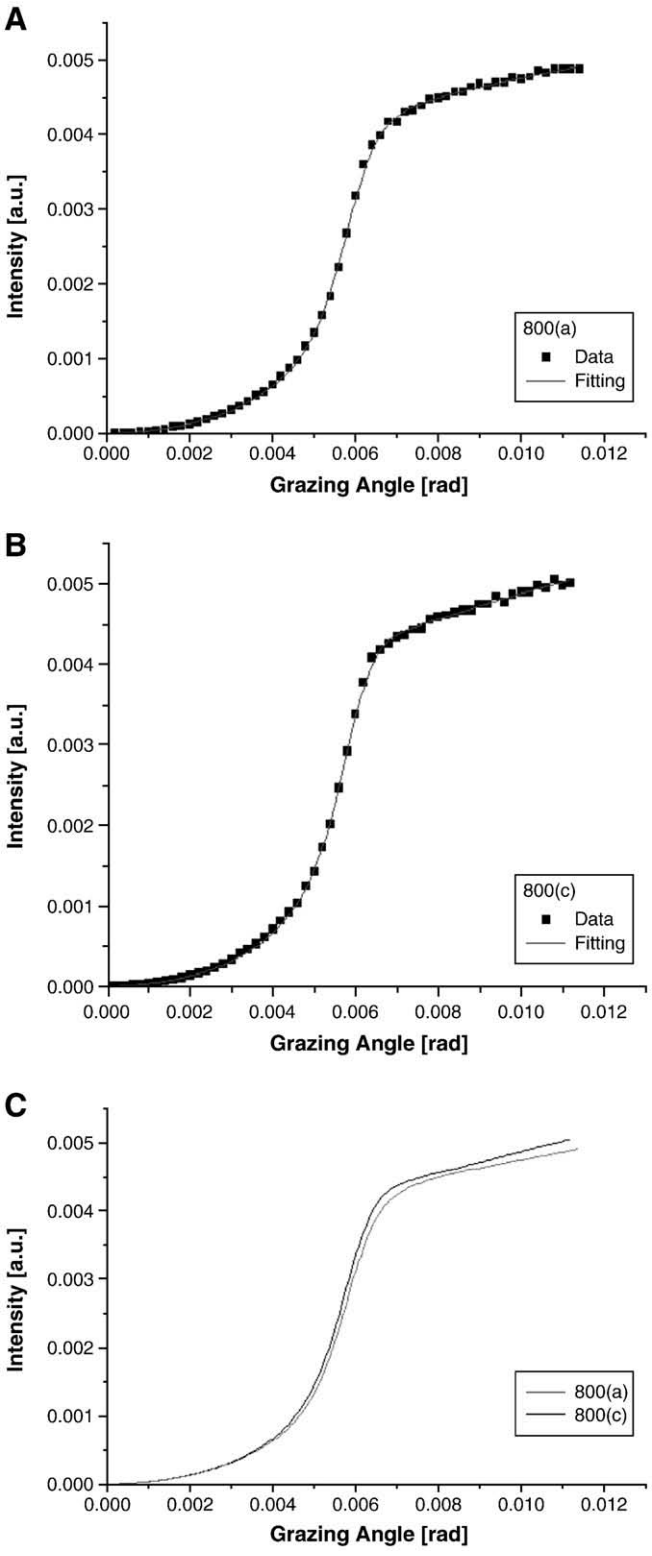

Fig. 5. (A) Experimental data of the sample with a surface layer of 800 Å, right after deposition. The solid line represents the fitting curve considering two layers. Layer 1: 4.6 g/cm³, 51 Å. Layer 2: 8.4 g/cm³, 486 Å. (B) Experimental data of the sample with a surface layer of 800 Å, after 30 min in oven at 65°. The solid line represents the fitting curve considering two layers. Layer 1: 4.9 g/cm³, 70 Å. Layer 2: 8.7 g/cm³, 470 Å. (C) A comparison of the fitted curves of (A) and (B).

Table 1
Compilation of fitted parameters for the different samples. Density in cm^2/g and depth in Å.

Surface layer	Treatment	Layer #1		Layer #2	
		Density	Depth	Density	Depth
190 Å	After deposition	5.9	16	8.4	180
	30 min at 65º	6.3	37	8.5	168
400 Å	After deposition	4.6	31	8.5	378
	30 min at 65º	4.9	53	8.6	356
800 Å	After deposition	4.6	51	8.4	486
	30 min at 65º	4.9	70	8.7	470

the sample with the surface layer of 400 Å, the fittings show the same characteristics of the sample of 190 Å, especially regarding the densities but with less consistency in the depths that, in this case, do not match so better the original depth. The sample with a surface layer of 800 Å shows a similar behavior than for the previous sample, except that the sum of the thicknesses of the 2 layers does not match the nominal thickness. This could be due to a possible error in the sample preparation during the evaporation of Cu on the Si surface in combination with the fact that the layer is too thick and behaves as a substrate.

Several models of surface layers were evaluated, considering different numbers of layers. The calculation revealed that when more than three layers were used, the fittings showed inconsistent and imprecise results with high variations in the fitting parameters.

The reason for these problems relies on the basis and fundamentals of the stratified model when it is applied to a continuously varying medium. The stratified model is based on the interference effect of the transmitted and reflected waves in each interface, obtaining in this way the total intensity of the wave that exits from the medium. Expressions for travelling waves are described basically by:

$$A_\alpha \exp\left(-ikP_\alpha z_\alpha\right)$$

where A_α is the amplitude of the electric field in the αth layer, k is the wave number, P_α is the Fresnel's parameter in the αth layer and z_α is the depth in the αth layer. In this expression the homogeneity of the space is assumed, i.e., the spatial symmetry in the y,x-planes parallel to the external surface has to be preserved in order to avoid phase changes in the y,x-plane. On one hand, this fact is not necessarily true since it depends on the origin and/or the manner in which the continuous medium was created (ion implantation, surface oxidation, sputtering, etc.). On the other hand, and more important even, the stratified model requires interfaces to create transmitted and reflected waves through them. These fields will later interfere among them to produce the typical destructive/constructive pattern of waves. In a continuous medium there are not interfaces that split the beams; hence, there are not well defined transmitted or reflected waves to produce interference among each other. It is clear that, without well defined interfaces, the optical path of the waves inside the medium has random values and thus no interference effects can occur.

The calculations of this work demonstrate that increasing the number of layers produces inconsistent or unreliable results; they can generate probably good fittings but not with reasonably well fitted parameters. With a one-layer or a two-layer scheme, the calculations fit very well the experimental data but the information obtained about the depth profile have only a limited significance since the exact distribution of the oxidized copper cannot be given.

In several papers, the stratified method was used to reproduce a continuous depth profile by a non-linear fitting of the experimental data. In general, this procedure allows a good fit of the data, mostly because the fitting function has several parameters to adjust. Nevertheless, according to the comments above, this method is not reliable to obtain a precise characterization of the depth profile.

4. Conclusions

The different angular scans for each individual sample differ only slightly. The most significant variations are observed for the first measurement (after evaporation) and the last one (after the heating in oven).

Our results also show that the atmosphere oxidation is produced in the first instance of atmosphere exposition after the sputtering, and is increased only if the sample is heated. Finally, for surface layers thicker that 400 Å the layer is too thick and it behaves like a substrate.

The mathematical model worked correctly for a one-layer or two-layer schemes but shows inconsistencies for more complex schemes. This indicates that the stratified model is not appropriate for continuous media due to the nature of the theoretical assumptions on which the stratified model is based. To obtain a more precise and realistic description of the emitted fluorescence emerging from a surface with a continuous depth profile, more complex algorithms have to be implemented (see for example Ref. [10]).

Acknowledgement

This work was partially supported by the LNLS — National Synchrotron Light Laboratory, Brazil.

References

[1] Y. Yoneda, T. Horiuchi, Optical flats for use in X-ray spectrochemical microanalysis, Rev. Sci. Instrum. 42 (1971) 1069–1070.
[2] J.M. Bloch, M. Sansone, F. Rondelez, D.J. Peifer, P. Pincus, M.W. Kim, P.M. Eisenberger, Concentration profile of a dissolved polymer near the air–liquid interface: X-ray fluorescence study, Phys. Rev. Lett. 54 (1985) 1039–1042.
[3] R.S. Becker, J.A. Golovchenko, J.R. Patel, X-ray evanescent-wave absorption and emission, Phys. Rev. Lett. 50 (1983) 153–156.
[4] L.D. Landau, E.M. Lifschitz, Electrodynamics of Continuous Media, Pergamon, Oxford, 1981.
[5] G.H. Vineyard, Grazing-incidence diffraction and the distorted-wave approximation for the study of surfaces, Phys. Rev. B26 (1982) 4146–4159.
[6] René E. Grieken, Andrej A. Markowicz (Eds.), Handbook of X-Ray Spectrometry: Methods and Techniques, Marcel Dekker, Inc, New York, 1993.
[7] L.G. Parrat, Surface studies of solids by total reflection of X-rays, Phys. Rev. 95 (1954) 359–369.
[8] R.D. Pérez, H.J. Sánchez, M. Rubio, Theoretical model for the calculation of interference effects in TXRF and GEXRF, X-Ray Spectrom. 30 (2001) 292–295.
[9] R.D. Pérez, H.J. Sánchez, M. Rubio, Efficient calculation method for Glancing Angle X-Ray Techniques, X-Ray Spectrom. 31 (2002) 296–299.
[10] S.M.P. Smolders, H.P. Urbach, On the determination of dopant-concentration profiles by grazing emission X-ray fluorescence spectroscopy using the maximum-entropy method, J. Eng. Math. 43 (2002) 115–134.
[11] C.A. Pérez, M. Radtke, H.J. Sánchez, H. Tolentino, R.T. Neuenshwander, W. Barg, M. Rubio, M.I.S. Bueno, I.M. Raimundo, J.J.R. Rohwedder, Synchrotron Radiation X-Ray Fluorescence at the LNLS: beamline instrumentation and experiments, X-Ray Spectrom. 28 (1999) 320–326.
[12] T. Shiraiwa, N. Fujino, Theoretical calculation of fluorescent X-ray intensities in fluorescent X-ray spectrochemical analysis, Jpn. J. Appl. Phys. 5 (1966) 886–899.
[13] R.D. Pérez, H.J. Sánchez, M. Rubio, C.A. Pérez, Mathematical model for evaluation of surface analysis data by total reflection, X-Ray Spectrom. 28 (1999) 342–347.